

Single top and Higgs associated production at the LHC

Vernon Barger,¹ Mathew McCaskey,¹ and Gabe Shaughnessy^{2,3}

¹*Department of Physics, University of Wisconsin, Madison, WI 53706*

²*Northwestern University, Department of Physics and Astronomy, Evanston, IL 60208 USA*

³*HEP Division, Argonne National Lab, Argonne IL 60439 USA*

Abstract

We study the production of a Standard Model (SM) Higgs boson in association with a single top quark and either a light jet or W -boson at the LHC with a center of mass energy of 14 TeV. Due to the destructive interference of the contributing SM diagrams, the value of the top Yukawa coupling and the sign of the $WW h$ coupling may be probed for Higgs masses above 150 GeV where WW and ZZ are the dominant Higgs decays. We consider Higgs masses of $m_h = 120, 150, 180$, and 200 GeV and devise experimental cuts to extract the signal from SM backgrounds and measure the top Yukawa coupling.

I. INTRODUCTION

The Higgs boson associated with spontaneous electroweak symmetry breaking (EWSB) is one of the most important anticipated discoveries in modern particle physics. To this end, several Higgs boson production and decay channels have been extensively studied. Searches at the Fermilab Tevatron have recently excluded a Standard Model (SM) Higgs boson in the mass range of 160-170 with 95% confidence GeV [1], wherein $H \rightarrow WW^{(*)}$ is the dominant decay mode. Simulations for upcoming searches by the ATLAS and CMS detectors at the LHC [2, 3, 4] at 14 TeV indicate that a 5 sigma Higgs discovery is achievable with 10 fb^{-1} luminosity over the full SM Higgs boson mass range of interest, 110 - 800 GeV [5].

The upper bound of this mass range comes from the requirement that the electroweak (EW) theory is consistent up to a certain energy scale Λ . By analyzing the running of the quartic coupling in the Higgs potential up to Λ , an upper bound can be put on the coupling and hence the Higgs mass itself [6, 7]. If electroweak theory is consistent up to the Plank scale this upper bound is $\lesssim 200 \text{ GeV}$ [8]. Lowering the energy scale of new physics to $\Lambda = 1 \text{ TeV}$, accessible at the LHC, the upper bound on the SM Higgs mass increases to $\lesssim 800 \text{ GeV}$. The lower bound on the Higgs mass arises from the stability requirement of the Higgs potential. Radiative corrections associated with top-quark loops can destabilize the minimum of the Higgs potential if the Higgs mass is $< 50 \text{ GeV}$ at $\Lambda = 1 \text{ TeV}$ and $< 100 \text{ GeV}$ at the Planck scale [7, 9, 10]. A SM Higgs with mass less than 114 GeV is excluded by LEP 2 searches [11].

Beyond Higgs discovery, measurements of the Higgs couplings to other SM particles will test the fundamental properties of the Higgs [12, 13, 14, 15, 16]. Its couplings to the W and Z bosons are definitive tests of the SM, since both the W , Z masses and the WWh , ZZh couplings are determined by the vacuum expectation value (vev) of the neutral physical Higgs state. The relation of the W -boson mass to the vev including the radiative corrections from the top quark and Higgs boson loops is [17, 18, 19]¹

$$M_W^2 = \frac{\pi\alpha}{\sqrt{2}G_F s_w^2} \left[1.07 - \frac{G_F}{\sqrt{2}} \frac{3}{8\pi^2} \left(\frac{c_w^2}{s_w^2} \right) m_t^2 + \frac{\alpha}{\pi s_w^2} \frac{11}{48} \left[\log \left(\frac{M_h^2}{M_Z^2} \right) - \frac{5}{6} \right] \right] \quad (1)$$

where c_w and s_w are the cosine and sine of the weak mixing angle, respectively.

¹ This approximation is only valid for $m_h \gg M_Z$.

Measurements of the Yukawa couplings of the Higgs boson to the top and bottom quarks will show whether the third generation quark masses are also generated by the SM Higgs. More generally, measurements of the weak boson and fermion couplings can differentiate Higgs mechanisms that involve more than one Higgs doublet [16].

The principal SM Higgs production mechanisms are Z and W Higgstrahlung [20, 21, 22], Weak Boson Fusion [23, 24, 25, 26], gluon fusion [27, 28, 29], and production in association with a top quark pair [30, 31, 32, 33, 34, 35, 36, 37]. The gluon fusion process occurs at loop level and as such that prediction is dependent on the contributions of the virtual SM particles in the loops, dominated by the top-quark loop. The SM Higgs boson decay branching fractions depend sensitively on the Higgs mass, with the $WW^{(*)}$ and $ZZ^{(*)}$ decay modes dominating above the WW threshold and $b\bar{b}$ dominating at lower Higgs masses.

In principle, the top quark Yukawa coupling may be probed through Higgs production with an associated top, anti-top quark pair [30, 31, 32, 33, 34, 35, 36, 37, 38] and Higgs production via gluon fusion [27, 28, 29]. These processes require the high energy and high luminosity of the LHC. Early studies done to isolate the Higgs signal in the $t\bar{t}h$ production process found optimistic conclusions but more refined simulations now indicate that it will be very difficult to isolate this signal from SM backgrounds for a Higgs mass in the range of 120-200 GeV [2]. However, a more optimistic assessment has recently been reached in Ref. [38].

Our interest in this paper is the potential LHC measurement of the top Yukawa coupling through Higgs production in association with a single top quark. Previous simulations of this process and its SM backgrounds [39, 40, 41, 42, 43, 44, 45] have focused on SM Higgs masses for which the $b\bar{b}$ decay mode dominates. We revisit the $H \rightarrow b\bar{b}$ channel and reproduce the results of previous simulations that this signal is buried by backgrounds. Thereafter we focus on the equally interesting case where the Higgs decays dominantly to the $WW^{(*)}$ and $ZZ^{(*)}$ final states.

The single top-Higgs channel provides a unique way to test the SM prediction of the sign of the WWh coupling due to the interference of two contributing Feynman diagrams [44]: see Section II. We discuss our collider simulations and acceptance cuts to extract the $H \rightarrow WW^{(*)}, ZZ^{(*)}$ signals from SM backgrounds in Sections III and IV respectively. Finally, in Section V we quantitatively evaluate the interference between the contributing diagrams to test the sign of the WWh coupling.

We base our study on the center of mass design energy of 14 TeV and an integrated luminosity of 300 fb^{-1} for each of the two detectors (ATLAS and CMS). The super-LHC would deliver ten times the luminosity of the LHC [5] and accordingly should increase the sensitivity to the process of interest here.

II. SINGLE TOP QUARK AND HIGGS ASSOCIATED PRODUCTION

Single top production has been studied extensively both in the SM and models beyond the SM [46, 47, 48, 49, 50, 51, 52, 53, 54]. In the SM a single top quark can be produced in association with either a light quark, W -boson, or bottom quark. The Feynman diagrams for these three processes are given in Fig. 1.

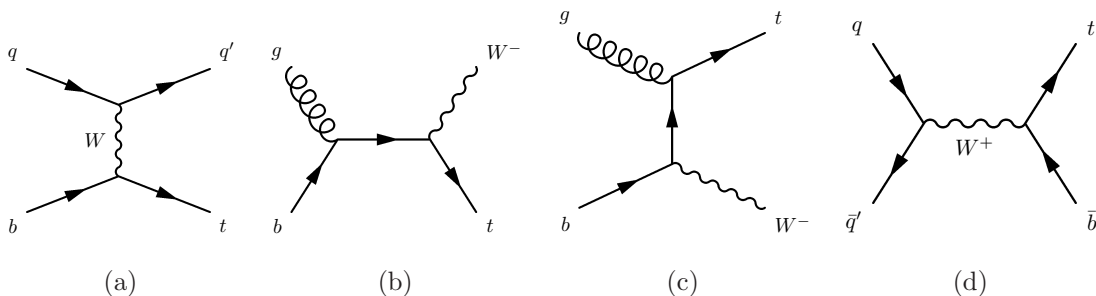


FIG. 1: Feynman diagrams for single top production at the LHC with various associated particles. (a) The t -channel W exchange with an associated light jet. (b-c) The s and t channel diagrams with an associated W -boson. (d) The s -channel W exchange with an associated b jet. Similar diagrams exist for anti-top quarks in the final state.

The single top production process is of electroweak strength. Nevertheless, at the LHC the cross section is within a factor of 5 of $t\bar{t}$ production via the strong process $gg \rightarrow t\bar{t}$. We concentrate on the single top and single anti-top channels with an associated light quark and associated W -boson, since those processes have the largest cross sections: see Table I. In addition, we note that the large $t\bar{t}$ background process, largely from $gg \rightarrow t\bar{t}$ at LHC energies, can mimic the $t\bar{b}$ process with a failed lepton tag.

Several calculations have been made of next-to-leading order (NLO) and next-to-next-to-leading order (NNLO) corrections to single top production at the LHC [57, 58, 59, 60, 61, 62, 63, 64]. These corrections can increase the production cross section by as much as 50% in the case of the tW channel; the corrections are more modest for the tq' and $t\bar{b}$ channels. The

$\sigma(pp \rightarrow tj)$	120 pb	$\sigma(pp \rightarrow \bar{t}j)$	67 pb
$\sigma(pp \rightarrow tW^-)$	31 pb	$\sigma(pp \rightarrow \bar{t}W^+)$	31 pb
$\sigma(pp \rightarrow tb)$	4.0 pb	$\sigma(pp \rightarrow \bar{t}\bar{b})$	2.4 pb
$\sigma(pp \rightarrow t\bar{t})$	582 pb		

TABLE I: Comparison of top pair and single top production cross sections at 14 TeV center of mass energy. All of the cross sections here and in the rest of our paper were calculated using the MadGraph [55] software package with the CTEQ6L parton distribution functions [56]. All cross sections were calculated to have a statistical error less than 1%.

higher order QCD corrections to single top-Higgs associated production will be similar. For this study we conservatively concentrate on the contributions from leading order diagrams without QCD K-corrections.

To produce a SM Higgs in association with a single top quark, a Higgs boson is radiated from each of the massive particles in the Feynman diagrams associated with single top production. Higgs radiation from a b quark (or any other light quark) is suppressed by the small Yukawa coupling and the intermediate quark being far off-shell. Therefore, Higgs radiation from the W -boson and the top quark give the dominating contributions to the production cross section. The extended Feynman diagrams, including the sites where the Higgs is radiated, are given in Fig. II, with \times marking possible Higgs emissions.

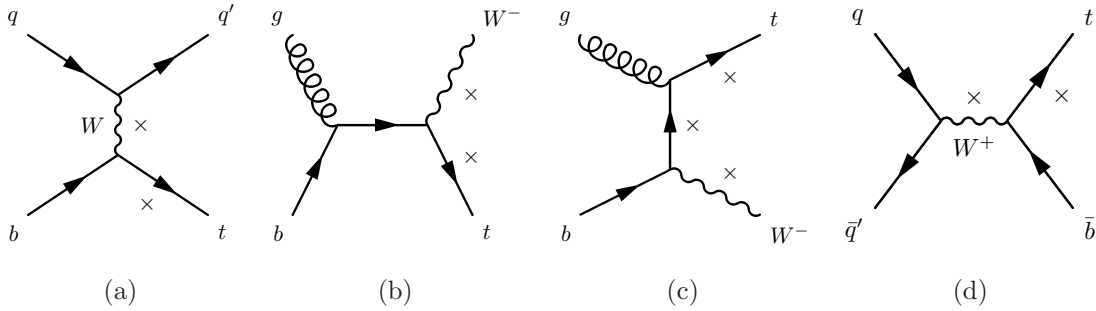


FIG. 2: Feynman diagrams contributing to the Higgs production with an associated single top. The diagrams are the same as the single top production but with a Higgs boson radiated from the W -boson or the top quark. The locations where the Higgs can be radiated is denoted by \times with only one radiated Higgs implied.

We consider Higgs masses of 120, 150, 180, and 200 GeV in our analysis. The low Higgs mass of 120 GeV, with $h \rightarrow b\bar{b}$ decay, has been studied previously in [39] and was shown to have insurmountable background contamination. The other Higgs mass cases have large branching fractions to weak bosons which potentially makes it easier to extract the signal from the background when one of the weak bosons decay leptonically. We calculate the production cross sections for the aforementioned Higgs masses and obtain the results given in Table II. The produced top (anti-top) quarks in association with a Higgs boson that is radiated from the $t(\bar{t})$ prefferentially have a right-handed (left-handed) polarization, due to the $V - A$ weak coupling and the chirality flip from the Higgs emission. The leptons from t_L and t_R semileptonic decays have different distributions, but the fact that both tops and anti-tops are produced makes it difficult to exploit the differences.

	$tjh \ \bar{t}jh$	$tW^-h \ \bar{t}W^+h$	$tbh \ \bar{t}bh$	$t\bar{t}h$
$m_h = 120 \text{ GeV}$	45 23	9.0 9.0	1.6 0.8	440
$m_h = 150 \text{ GeV}$	33 19	5.0 5.0	1.0 0.5	240
$m_h = 180 \text{ GeV}$	31 16	3.0 3.0	0.6 0.3	140
$m_h = 200 \text{ GeV}$	29 15	2.4 2.4	0.5 0.2	100

TABLE II: The cross sections (in fb) at 14 TeV of the SM Higgs production with an associated single top and the three possible final state particles for various Higgs mass choices. The cross section for the Higgs production with an associated top quark pair is included in the last column for comparison.

We calculate the branching fractions of the Higgs to SM particles using HDECAY [65] for the different Higgs masses. These results are given in Table III.

III. COLLIDER SIMULATIONS

The events used in our analysis were generated at tree level with the MadGraph [55] and Alpgen [66] packages using the CTEQ6L parton distribution functions [56]. We use a renormalization and factorization scale consistent with Refs. [67, 68] given by

m_h (GeV)	$\text{BF}(h \rightarrow ZZ^{(*)})$	$\text{BF}(h \rightarrow WW^{(*)})$	$\text{BF}(h \rightarrow b\bar{b})$
120	0.015	0.138	0.673
150	0.082	0.693	0.168
180	0.059	0.933	0.005
200	0.253	0.743	0.003

TABLE III: Branching fractions of the Higgs to $ZZ^{(*)}$, $WW^{(*)}$, and $b\bar{b}$ pairs for the Higgs masses we study.

$$Q = \frac{1}{2} \sum_{i=t,h,W,Z} M_i. \quad (2)$$

To simulate the unweighted events at the parton level we apply energy and momentum smearing to the final state particles according to the usual prescription

$$\frac{\delta E}{E} = \frac{a}{\sqrt{E}} \oplus b, \quad (3)$$

where $a = 0.5, 0.1$ and $b = 0.03, 0.007$ for jets and leptons respectively. We require the final state particles to have $p_T > p_T^{min}$ and $|\eta| < \eta_{max}$, where p_T^{min} and η_{max} are defined as

$$\begin{aligned} p_T^{\ell=e,\mu} &> 20 \text{ GeV}, & |\eta_e| &< 2.4, & |\eta_\mu| &< 2.1, \\ p_T^\tau &> 15 \text{ GeV}, & |\eta_\tau| &< 2.5, \\ p_T^{j,b} &> 20 \text{ GeV}, & |\eta_j| &< 4.5, & |\eta_b| &< 2.0. \end{aligned} \quad (4)$$

Jets are defined at the parton level. We also require final state particles to be isolated in the detector. Our isolation requirement is a minimum ΔR between all final leptons and jets as defined by

$$\Delta R = \sqrt{\Delta\eta^2 + \Delta\phi^2}. \quad (5)$$

where $\Delta\eta$ is the rapidity gap and $\Delta\phi$ is the azimuthal angle gap between the particle pair. We impose the following criteria for ΔR separations:

$$\Delta R(jj, j\ell, \ell\ell) > 0.4. \quad (6)$$

Along with these acceptance and isolation criteria, we impose a tagging efficiency of 0.6, 0.9, and 0.4 for final state b jets, leptons (electrons and muons), and taus respectively. We also include b and τ mis-tagging rates as follows:

$$\varepsilon_{c \rightarrow b} = 0.1 \text{ for } p_T > 50 \text{ GeV} \quad (7)$$

$$\varepsilon_{j \rightarrow b} = \begin{cases} \frac{1}{50} & \text{for } p_T > 250 \text{ GeV} \\ \frac{1}{150} \left(\frac{2(p_T - 100)}{150} + 1 \right) & \text{for } 100 \text{ GeV} < p_T < 250 \text{ GeV} \\ \frac{1}{150} & \text{for } p_T < 100 \text{ GeV} \end{cases} \quad (8)$$

$$\varepsilon_{q \rightarrow \tau} = \begin{cases} \frac{1}{30} & \text{for } 15 \text{ GeV} < p_T < 30 \text{ GeV} \\ \frac{1}{100} & \text{for } 30 \text{ GeV} < p_T \end{cases} \quad (9)$$

These tagging and mis-tagging efficiencies are consistent with the values in the latest ATLAS TDR [2].

IV. COLLIDER STUDY

A. Backgrounds

The main Higgs decay channels are weak boson or bottom quarks pairs (See Table III). The further hadronic decay of the weak bosons leads to at most four jets from the Higgs, neglecting jets from final state radiation. With the Higgs produced in conjunction with a top quark and either a light jet or a W -boson, the hadronic decays of these particles lead up to a total of eight or nine jets respectively in the final state. The QCD background with the largest cross section is a $t\bar{t}$ pair produced with up to two extra jets. A more complete set of backgrounds include electroweak processes that give similar number of final state leptons and jets. We include $t\bar{t}V$, $t\bar{t}Vj$, $tV\bar{V}$, $VV\bar{V}$, $VV\bar{V}j$, $VV\bar{V}V$, and $VV\bar{V}Vj$ in our list of background events, where $V = W, Z$. A summary of the cross sections of all background processes considered is given in Table IV. The QCD and EW background processes are given along with their cross sections and maximum numbers of jets that can appear in the final state.

Process	$t\bar{t}$	$t\bar{t}j$	$t\bar{t}jj$	$t\bar{t}Vj$	$t\bar{t}V$	$3Vj, 4Vj$	$3V, 4V$	tVV
$\sigma(\text{pb})$	530	440	300	1.2	1.1	.37	.27	.12
$\max(N_{jets})$	6	7	8	9	8	7 – 9	6 – 8	7

TABLE IV: Cross sections for SM background processes included in our analysis for the same parton distribution functions and acceptance cuts as our signal calculations. These cross sections and maximum number of jets enable us to decide which background channels will be important for each of the signal processes.

B. $h \rightarrow b\bar{b}$ Channel

The tjh signal with a Higgs mass of 120 GeV has been studied in Ref [39] for the SM and in Ref [69] for the little Higgs model. For $h \rightarrow b\bar{b}$ at $m_h = 120$ GeV ², the primary backgrounds are $t\bar{t}$ and $t\bar{t}j$ for the tjh signal and $t\bar{t}j$ and $t\bar{t}jj$ for the tWh signal.

To reduce the QCD backgrounds we require a tagged lepton from the semileptonic decay of the associated top quark. Because the tjh process is a t -channel W exchange the associated light jet will nominally have high rapidity and high p_T . We therefore make a cut requiring a light quark jet (i.e. not a b -tagged jet) to have an absolute pseudorapidity greater than 2 and a p_T greater than 50 GeV. We reconstruct the Higgs mass from two of the three tagged b jets and require the invariant mass of these two b -jets to be within a 40 GeV window centered around the Higgs mass to allow for resolution of smeared jets. After imposing these acceptance cuts we find the signal is still overwhelmed by QCD backgrounds as previously found in Ref. [39].

In the tWh search we can obtain the required tagged lepton from the associated $W \rightarrow \ell\nu$ decay. This allows us to reconstruct the top quark using a third tagged b -jet and two lighter jets from the $W \rightarrow q\bar{q}$ decay. We take a mass window of 40 GeV for the reconstruction of both the Higgs (from two b -jets) and the top (from a b -jet and two light jets) and a window of 20 GeV for the reconstruction of the W -boson from the top decay. Again we find that the signal is overwhelmed by QCD backgrounds after applying all of our cuts with an integrated luminosity of 600 fb⁻¹.

² We cannot exploit the loop induced decay $H \rightarrow \gamma\gamma$ due to its low branching fraction ($\mathcal{O}(10^{-3})$).

C. $h \rightarrow WW^{(*)}$

Higgs masses with $m_h \gtrsim 2M_W$ have large branching fractions to two W bosons (see Table III). The subsequent W -boson decays may increase the number of final state particles and the increase in the number of intermediate particles to reconstruct helps make the backgrounds manageable. In events for which both W -bosons decay leptonically we could use cuts to exploit the spin-correlations of the leptons; because both W -bosons originate from a spin-0 Higgs and the $V - A$ coupling of the W -bosons decays make it likely that the two leptons will be detected close together [70]. Unfortunately, the square of the leptonic W branching fraction renders the spin-correlated lepton signal too small to be useful with our small signal cross sections.

For the tjh signal we require a single tagged lepton to reduce the QCD backgrounds. We consider the case that the lepton originates from the top quark decay to allow full reconstruction of the Higgs. We require a light jet to have a high rapidity and high p_T because of the nature of the t channel W exchange of the signal process. We can reconstruct two W -bosons from the Higgs decay (in the case of the 150 GeV Higgs only the real W -boson can be reconstructed) and the Higgs mass from the two reconstructed W -bosons. Still, we find that for all the Higgs choices the tjh signal is overwhelmed by backgrounds.

For the tWh signal we next consider the case where the tagged lepton comes from the decay of the associated W -boson. With both the top quark and Higgs decaying to jets we can reconstruct the Higgs boson mass from 4 light jets. In this reconstruction we require that the invariant mass of the four jets must be within 20 GeV of the Higgs mass. To justify this mass window we take a sample of signal events and plot the invariant mass of 4 light jets under the condition that the remaining 3 jets (one of which is a b -jet) reconstruct the top quark. Fig. 3 shows a noticeable signal peak centered around 150 GeV within 20 GeV of the Higgs mass.

Next we reconstruct the top quark from the 3 remaining jets of the signal by requiring the invariant mass of the jets to be within 20 GeV of the top mass. To further reduce backgrounds we reconstruct the W -boson from the top quark decay and the real W -bosons from the Higgs decay (In the $m_h = 150$ GeV case only one of the W is reconstructable.). The Feynman Diagrams for this signal are shown in Fig. 4.

With these cuts we obtain the event rates given in Table V. Because the tWh signal yields

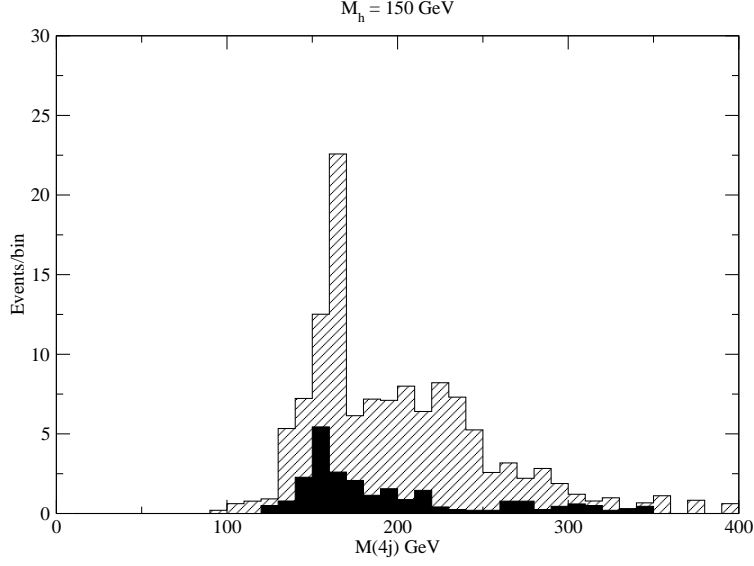


FIG. 3: Reconstruction of a 150 GeV Higgs mass via the invariant mass of 4 jets using 600 fb⁻¹ of data. A peak at 150 GeV is visible in the signal (black) within 20 GeV of the Higgs mass. The background (hatched) peak is a combinatoric result of the cuts.

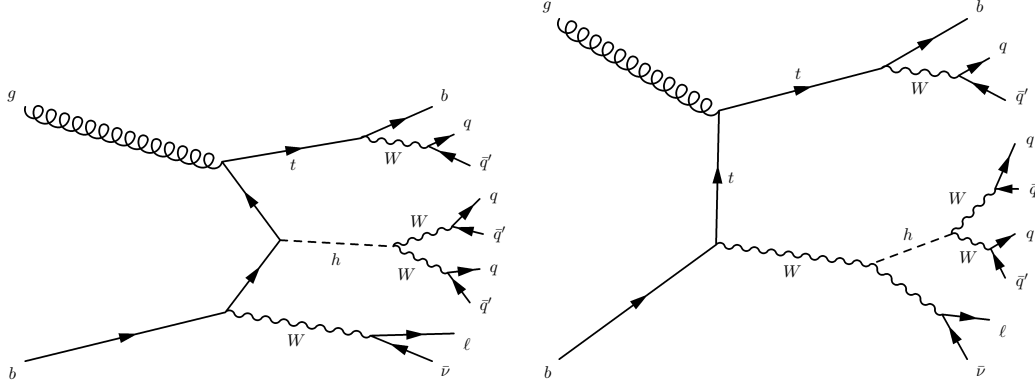


FIG. 4: Extended Feynman diagrams for the tWh signal where the $h \rightarrow WW$ decay channel is shown.

one more final state jet than the tjh signal, many of the QCD backgrounds that overwhelmed the tjh signal do not pass our set of cuts. The dominant background for this process is $t\bar{t}Vj$. With 600 fb⁻¹ of integrated luminosity we obtain a signal statistical significance $S/\sqrt{(S+B)}$ of 1.6, 1.2, and 0.7 for 150, 180, and 200 GeV Higgs masses respectively. The smaller statistical significance for the signal of the 200 GeV Higgs mass can be attributed to the smaller production cross section and a larger number of background events passing

Signal Event Rate at 600 fb ⁻¹ for 7j + 1ℓ:	$m_h = 150$ GeV 270 events			$m_h = 180$ GeV 230 events			$m_h = 200$ GeV 140 events		
Cut	S	B	$\frac{S}{\sqrt{S+B}}$	S	B	$\frac{S}{\sqrt{S+B}}$	S	B	$\frac{S}{\sqrt{S+B}}$
tagging: 7 j, 1ℓ, 1 b	67	20100	0.5 ± 0.1	64	20100	0.4 ± 0.1	50	20100	0.4 ± 0.1
$ M_{4j} - m_h < 20$ GeV	44	2000	1.0 ± 0.2	45	5200	0.6 ± 0.1	41	7600	0.5 ± 0.1
$ M_{bjj} - m_t < 20$ GeV	24	390	1.2 ± 0.3	26	1100	0.8 ± 0.2	23	1800	0.5 ± 0.1
$ M_{2j(top)} - M_W < 10$ GeV	21	160	1.6 ± 0.3	25	520	1.1 ± 0.2	17	890	0.6 ± 0.1
$ M_{2j(Higgs)} - M_W < 20$ GeV	20	150	1.5 ± 0.3	23	320	1.2 ± 0.3	16	580	0.7 ± 0.2

TABLE V: Cuts used to extract the tWh signal with $h \rightarrow WW^{(*)} \rightarrow$ jets for Higgs masses of 150, 180, and 200 GeV. The event rates include the appropriate branching fractions for a final state of 7 jets and 1 lepton. With each sequential cut the number of signal and background events that pass each sequential cut are given along with the resulting statistical significance of the signal. The statistical significance uncertainty is given by the propagated poisson uncertainties in the signal (S) and background (B) events.

the Higgs mass reconstruction cut.

D. $h \rightarrow ZZ^{(*)}$

Though the branching fraction of $h \rightarrow ZZ^{(*)}$ is smaller than the branching fraction of $h \rightarrow WW^{(*)}$ (Table III), the $ZZ^{(*)}$ signal is much easier to separate from SM backgrounds. If one of the Z bosons from the Higgs decays leptonically then we can reconstruct that Z very precisely because the lepton energy smearing is small (Eq. 3). This precise reconstruction of the Z boson greatly reduces the QCD backgrounds ($t\bar{t}$, $t\bar{t}j$, $t\bar{t}jj$, etc.) as it effectively requires a Z boson to be on-shell. For the second Z we require two jets to have an invariant mass within a 20 GeV window centered around M_Z , except for a 150 GeV Higgs where we can only reconstruct one of the Z bosons as the other will be off-shell. The two pairs of leptons and jets reconstruct the Higgs mass by requiring the invariant mass of the 2 jets and 2 leptons to be within 10 GeV of the Higgs mass. Fig. 5 illustrates why this mass window was chosen as this mass distribution shows a sharp peak in the invariant mass of the 2 jets and 2 leptons centered around the Higgs mass.

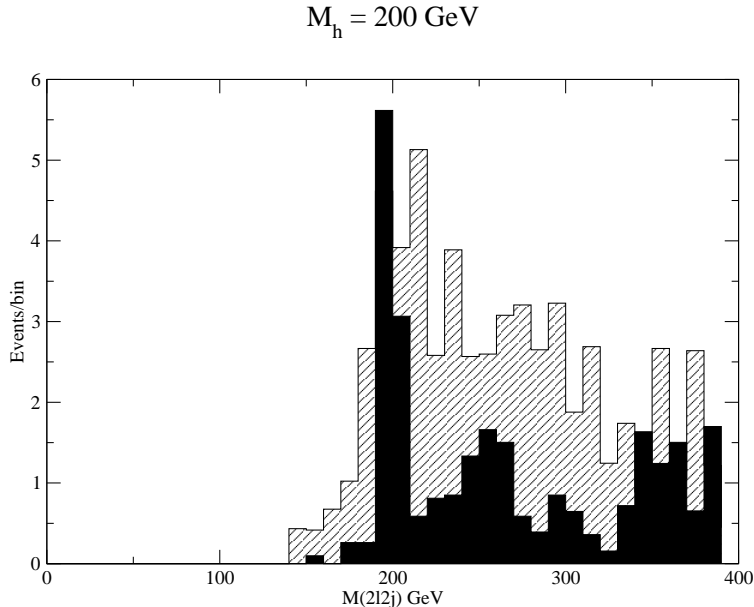


FIG. 5: Reconstruction of a 200 GeV Higgs mass from the invariant mass of 2 leptons and 2 jets using 600 fb^{-1} of data. Signal events are denoted by black histograms and background events by the hatched histogram. With each event plotted the lepton and jet pairs both reconstruct a Z boson and a top quark is reconstructed from 2 other light jets and a b -tagged jet. A peak at 200 GeV is visible within 10 GeV of the Higgs mass.

Next we reconstruct the top from a b jet and two other light jets. Finally, we once again tag a jet with high rapidity and high p_T . For the highest rapidity jet, we impose a minimum rapidity of 2.5. The results of this series of cuts are given in Table VI. It can be seen that this channel produces favorable results for extracting the Higgs signal when the Higgs has an appreciable branching fraction to ZZ . This favors the 200 GeV and 150 GeV cases. The 180 GeV Higgs mass is above the WW threshold and below the ZZ threshold so the decay to WW dominates. For even larger Higgs masses, the branching fraction to ZZ asymptotically approaches roughly 33%. For $m_h = 200 \text{ GeV}$ we obtain a statistical significance of 3.9σ with 600 fb^{-1} of integrated luminosity. The diagram for this process that gives the best detection significance is shown in Fig 6.

The tWh signal with $H \rightarrow ZZ^{(*)}$ cannot be used as effectively. The tWh signal with 600 fb^{-1} of integrated luminosity gives an order of only 10 events before acceptance and isolation cuts. Moreover this signal is dominated by the $t\bar{t}Zj$ background.

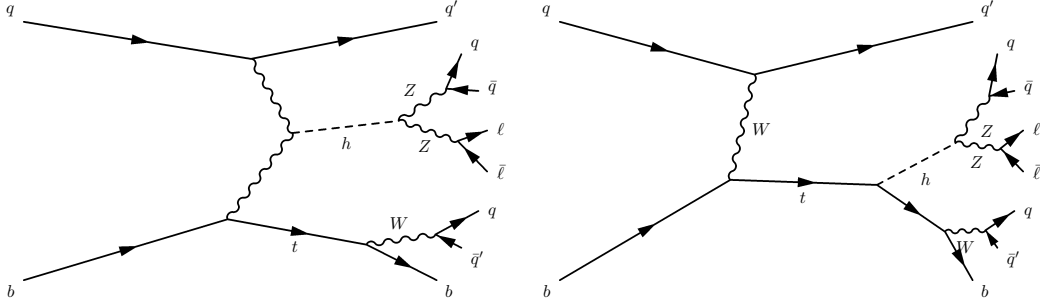


FIG. 6: Extended Feynman diagrams for the tjh signal where the $h \rightarrow ZZ$ decay channel is shown.

Signal Event Rate at 600 fb^{-1} for $6j + 2\ell$:	$m_h = 150 \text{ GeV}$ 84 events			$m_h = 180 \text{ GeV}$ 51 events			$m_h = 200 \text{ GeV}$ 216 events		
Cut	S	B	$\frac{S}{\sqrt{S+B}}$	S	B	$\frac{S}{\sqrt{S+B}}$	S	B	$\frac{S}{\sqrt{S+B}}$
tagging: $6j, 2\ell, \leq 1b$	11	1500	0.3 ± 0.1	9	1500	0.2 ± 0.1	53	1500	1.3 ± 0.2
$ M_{\ell\ell \text{ and } jj} - M_Z < 10 \text{ GeV}$	7	1400	0.2 ± 0.1	7	1400	0.2 ± 0.1	53	1400	1.4 ± 0.2
$ M_{bjj} - m_t < 20 \text{ GeV}$	6	1000	0.2 ± 0.1	4	1000	0.1 ± 0.1	45	1000	1.4 ± 0.2
$ M_{2j2\ell} - m_h < 10 \text{ GeV}$	5	28	0.9 ± 0.4	4	100	0.4 ± 0.2	41	180	2.8 ± 0.5
$ \eta_j > 2.5$	3	6	1.0 ± 0.6	2	20	0.3 ± 0.2	35	46	3.9 ± 0.7

TABLE VI: Table of the cuts used to extract the tjh signal with $h \rightarrow ZZ^{(*)}$ decay for Higgs masses of 150, 180, and 200 GeV. The event rates include the appropriate branching fractions to obtain a final state of 6 jets and 2 leptons. The number of signal and background events that pass the cut are given as well as the resulting statistical significance. For a Higgs mass of 200 GeV a statistical significance of 3.9σ is obtained with an integrated luminosity of 600 fb^{-1} .

V. CONSTRAINTS ON BEYOND THE SM COUPLINGS

The two contributing diagrams to Higgs production with a single top are proportional to the top Yukawa and the $WW h$ coupling, respectively. Therefore, the interference between these two diagrams depends on the sign of the $WW h$ coupling which allows a unique test of the SM prediction for this sign [44].

To illustrate, we parameterize the top Yukawa and gauge boson couplings as

$$y_t = c_t y_t^{SM}, \quad (10)$$

$$g_{WWh} = c_w g_{WWh}^{SM}, \quad (11)$$

where $c_t > 0$ and $c_w = \pm 1$ such that $c_t = c_w = 1$ for the SM³. It is expected that with the luminosity we adopt for this study, the magnitude of the WWh coupling will be measured precisely in the WW fusion process [71]. However, there is no direct way of determining the sign of the WWh coupling via the partial width of $h \rightarrow W^+W^-$ ⁴. A sign change for the WWh coupling can occur in multi-Higgs doublet models if the VEV direction in ϕ_1, ϕ_2 space is anti-aligned to the physical Higgs state [16]. For unitarity, there must be a second Higgs boson whose coupling to the gauge bosons has a positive sign. Therefore, if a negative sign of the gauge boson coupling to the Higgs is found, an additional CP even Higgs boson must exist.

In the following exploration of the top Yukawa strength, we adopt an absolute WWh coupling equal to that of the SM. If a coupling departure from the SM is found, it will be a reduction if the model contains doublets and/or singlets.

In Fig. 7 we show the effect of changing the top Yukawa scaling with both signs for the WWh coupling on the various Higgs production mechanisms. A significant increase in the cross sections occurs when the sign of the WWh coupling is negative. For example, with the SM top Yukawa and $c_w = -1$ the cross sections for the tjh and tWh channels increases by a factor of approximately 10. Accordingly, the integrated luminosity needed for the measurement of c_t could be substantially less.

Such a change in the top Yukawa and gauge boson coupling may also change the distributions of the final state particles which may potentially influence the optimal cuts. To quantify this, we repeated the analyses in Section IV with several values of c_t (in intervals of 0.25) and signs of c_w . This allows us to find a range of c_t that yield a $> 3\sigma$ significance with 600 fb^{-1} of integrated luminosity. Table VII shows the ranges of c_t without the c_w sign change. When the sign of c_w is flipped we find a statistical significance above 3σ for both signals and all Higgs masses studied. This shows that the Higgs production with an associated single top can provide a definitive test of both the top quark Yukawa coupling

³ The top quark Yukawa coupling must be positive since its sign is also that of the fermion mass which is fixed by vacuum stability.

⁴ In principle, the loop induced decay of $h \rightarrow \gamma\gamma$ can provide this information [72], but this decay is also sensitive to other states in the loop that may include new physics contributions, potentially masking the interference effect.

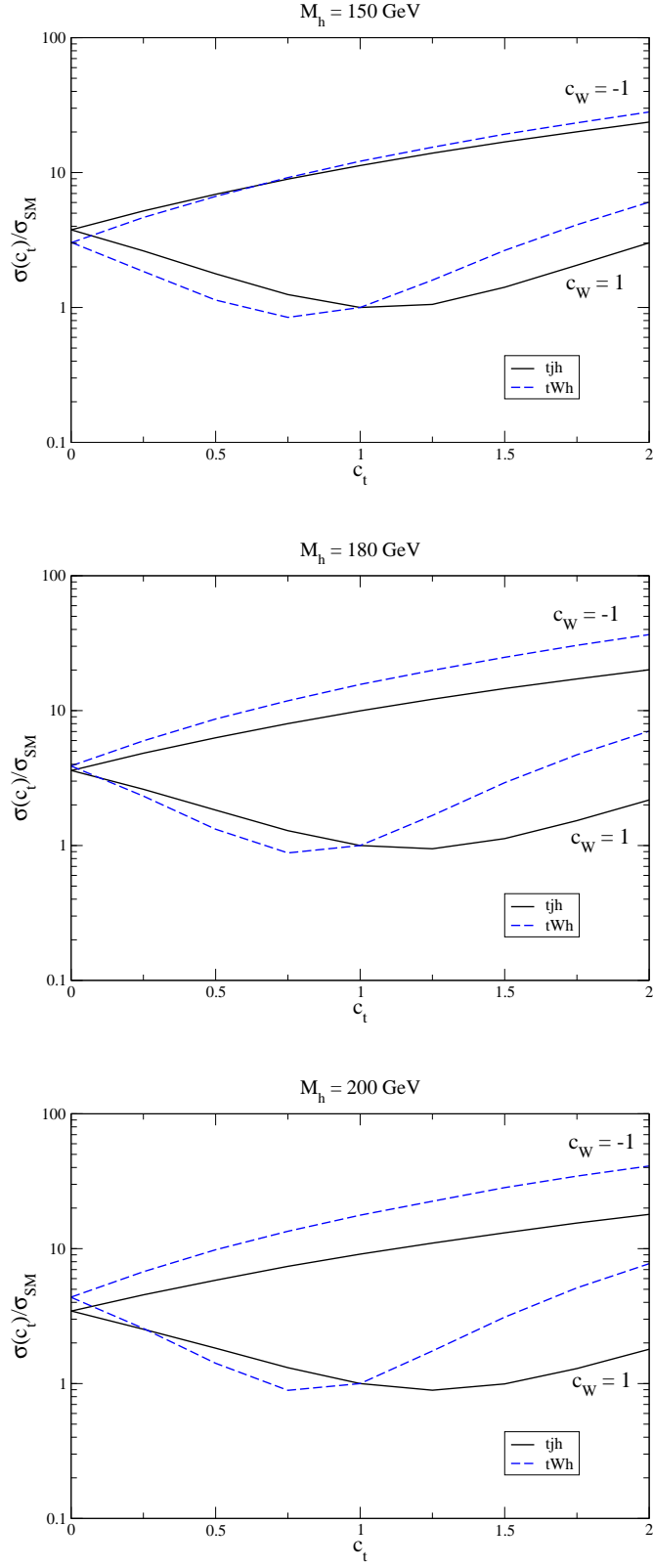


FIG. 7: Cross sections of Higgs production methods with associated top quarks with respect to the ratio of the top Yukawa coupling to the SM Yukawa coupling, c_t . The cross sections are scaled by that of the SM. There is a significant enhancement in the cross section when the sign of the $WW h$ coupling is negative.

and the sign of the WWh coupling.

Signal	$M_h = 150$ GeV	$M_h = 180$ GeV	$M_h = 200$ GeV
tjh ($c_w = 1$)	$1.75 < c_t$	$2.75 < c_t$	All c_t
tjh ($c_w = -1$)	All c_t	All c_t	All c_t
tWh ($c_w = 1$)	$c_t < 0.25, 1.50 < c_t$	$c_t < 0.25, 1.50 < c_t$	$1.75 < c_t$
tWh ($c_w = -1$)	All c_t	All c_t	$0.25 < c_t$

TABLE VII: Ranges of c_t above 3σ with 600 fb^{-1} of integrated luminosity using the same cuts in Section IV for both single top signals. The quoted boundaries are inclusive so it is possible to obtain 3σ significance with values of c_t slightly beyond these ranges. When the sign of the WWh is negative, most of the values of c_t yield a statistical significance above 3σ for both signals and all Higgs masses.

VI. CONCLUSIONS

In this paper we studied Higgs production with an associated single top quark for Higgs masses in the range of 120 GeV to 200 GeV. After making acceptance cuts to extract the signals from backgrounds, our conclusions are:

- The signal of the 120 GeV Higgs is overwhelmed by QCD backgrounds, consistent with the findings of Ref. [39].
- Overall, the best topology for isolating the signature of associated single top and Higgs production is via the $qb \rightarrow tjh$ subprocess with a hadronically decaying top quark and $h \rightarrow ZZ^{(*)} \rightarrow \ell^+\ell^- + jj$. For a SM Higgs with $m_h = 200$ GeV we found a significance of 3.9σ with 600 fb^{-1} of integrated luminosity.
- Further, we also found that these signals can be a definitive test for the overall sign for the WWh coupling. Specifically, if the WWh coupling is opposite in sign to the SM and the top quark Yukawa is the same as the SM, we found up to an order of magnitude increase in the overall event rate of single top and Higgs production at the LHC. This provides a statistical significance above 5σ for all of the Higgs masses studied.

- If the sign of the WWh coupling is negative, then a heavier scalar state must exist with a positive WWh coupling to unitarize the model. This would provide evidence for the existence of an extended Higgs sector.
- We have determined the ranges in which the top quark Yukawa can be probed to 3σ with 600 fb^{-1} of integrated luminosity assuming either sign of the WWh coupling; see Table VII.

Our study shows that single top plus Higgs production should be observable at the LHC with large integrated luminosity and provide important insights about the Higgs sector. More detailed studies including detector simulations are warranted.

VII. ACKNOWLEDGMENTS

We thank Qing-Hong Cao, Ian Low, Carlos Wagner and Ed Berger for helpful discussions. This work was supported in part by the U.S. Department of Energy under grants No. DE-FG02-95ER40896, DE-FG02-05ER41361, DE-FG02-08ER41531, and Contract DE-AC02-06CH11357, by the Wisconsin Alumni Research Foundation, and by the National Science Foundation grant No. PHY-0503584.

-
- [1] CDF and D0 Collaboration, *Combined CDF and DZero Upper Limits on Standard Model Higgs-Boson Production with up to 4.2 fb-1 of Data*, arXiv:0903.4001.
 - [2] ATLAS Collaboration, E. Richter-Was, *Acta Phys. Polon.* **B40**, 1909 (2009).
 - [3] CMS Collaboration, G. L. Bayatian *et al.*, CERN-LHCC-2006-001.
 - [4] CMS Collaboration, G. L. Bayatian *et al.*, *J. Phys.* **G34**, 995 (2007).
 - [5] M. L. Mangano, (2009), arXiv:0910.0030.
 - [6] T. Hambye and K. Riessellmann, *Phys. Rev.* **D55**, 7255 (1997).
 - [7] C. Quigg, (2009), arXiv:0905.3187.
 - [8] K. Tobe and J. D. Wells, *Phys. Rev.* **D66**, 013010 (2002).
 - [9] J. A. Casas, J. R. Espinosa, and M. Quiros, *Phys. Lett.* **B382**, 374 (1996).
 - [10] M. B. Einhorn and D. R. T. Jones, *JHEP* **04**, 051 (2007).
 - [11] LEP Working Group for Higgs boson searches, R. Barate *et al.*, *Phys. Lett.* **B565**, 61 (2003).

- [12] A. Djouadi *et al.*, (2000), hep-ph/0002258.
- [13] D. Zeppenfeld, R. Kinnunen, A. Nikitenko, and E. Richter-Was, Phys. Rev. **D62**, 013009 (2000).
- [14] A. Belyaev and L. Reina, JHEP **08**, 041 (2002).
- [15] ILC, G. Aarons *et al.*, (2007), arXiv:0709.1893.
- [16] V. Barger, H. E. Logan, and G. Shaughnessy, Phys. Rev. **D79**, 115018 (2009).
- [17] A. Sirlin, Phys. Rev. **D22**, 971 (1980).
- [18] W. F. L. Hollik, Fortschr. Phys. **38**, 165 (1990).
- [19] S. Dawson, AIP Conf. Proc. **1116**, 11 (2009).
- [20] S. L. Glashow, D. V. Nanopoulos, and A. Yildiz, Phys. Rev. **D18**, 1724 (1978).
- [21] J. Finjord, G. Girardi, and P. Sorba, Phys. Lett. **B89**, 99 (1979).
- [22] E. Eichten, I. Hinchliffe, K. D. Lane, and C. Quigg, Rev. Mod. Phys. **56**, 579 (1984).
- [23] D. R. T. Jones and S. T. Petcov, Phys. Lett. **B84**, 440 (1979).
- [24] R. N. Cahn and S. Dawson, Phys. Lett. **B136**, 196 (1984).
- [25] S. Asai *et al.*, Eur. Phys. J. **C32S2**, 19 (2004).
- [26] K. Cranmer, B. Mellado, W. Quayle, and S. L. Wu, ATL-COM-PHYS-2003-002 (2003) .
- [27] H. M. Georgi, S. L. Glashow, M. E. Machacek, and D. V. Nanopoulos, Phys. Rev. Lett. **40**, 692 (1978).
- [28] M. Duhrssen *et al.*, (2004), hep-ph/0407190.
- [29] M. Duhrssen *et al.*, Phys. Rev. **D70**, 113009 (2004).
- [30] R. Raitio and W. W. Wada, Phys. Rev. **D19**, 941 (1979).
- [31] Z. Kunszt, Nucl. Phys. **B247**, 339 (1984).
- [32] A. S. Bagdasaryan, R. S. Egorian, S. G. Grigorian, and S. G. Matinyan, Sov. J. Nucl. Phys. **46**, 315 (1987).
- [33] J. N. Ng and P. Zakarauskas, Phys. Rev. **D29**, 876 (1984).
- [34] F. Maltoni, D. L. Rainwater, and S. Willenbrock, Phys. Rev. **D66**, 034022 (2002).
- [35] S. Su and B. Thomas, (2008), arXiv:0812.1798.
- [36] R. Lafaye, T. Plehn, M. Rauch, D. Zerwas, and M. D'uhrrssen, (2009), arXiv:0904.3866.
- [37] A. V. Lipatov and N. P. Zotov, Phys. Rev. **D80**, 013006 (2009).
- [38] T. Plehn, G. P. Salam, and M. Spannowsky, (2009), 0910.5472.
- [39] F. Maltoni, K. Paul, T. Stelzer, and S. Willenbrock, Phys. Rev. **D64**, 094023 (2001).

- [40] J. L. Diaz-Cruz and O. A. Sampayo, Phys. Lett. **B276**, 211 (1992).
- [41] W. J. Stirling and D. J. Summers, Phys. Lett. **B283**, 411 (1992).
- [42] A. Ballestrero and E. Maina, Phys. Lett. **B299**, 312 (1993).
- [43] G. Bordes and B. van Eijk, Phys. Lett. **B299**, 315 (1993).
- [44] T. M. P. Tait and C. P. Yuan, Phys. Rev. **D63**, 014018 (2001).
- [45] J. M. Campbell, R. Frederix, F. Maltoni, and F. Tramontano, (2009), arXiv:0903.0005.
- [46] Q.-H. Cao, J. Wudka, and C. P. Yuan, Phys. Lett. **B658**, 50 (2007).
- [47] A. T. Alan, N. K. Pak, and A. Senol, Europhys. Lett. **83**, 21001 (2008).
- [48] D. Lopez-Val, J. Guasch, and J. Sola, PoS **RADCOR2007**, 042 (2007).
- [49] J. A. Aguilar-Saavedra, Nucl. Phys. **B804**, 160 (2008).
- [50] X. Wang, Y. Zhang, H. Jin, and Y. Xi, Nucl. Phys. **B810**, 226 (2009).
- [51] R. A. Coimbra *et al.*, Phys. Rev. **D79**, 014006 (2009).
- [52] G. D. Kribs, A. Martin, and T. S. Roy, JHEP **06**, 042 (2009).
- [53] T. Plehn, M. Rauch, and M. Spannowsky, (2009), arXiv:0906.1803.
- [54] T. M. Aliev and K. O. Ozansoy, (2009), arXiv:0905.1597.
- [55] J. Alwall *et al.*, JHEP **09**, 028 (2007).
- [56] J. Pumplin, A. Belyaev, J. Huston, D. Stump, and W. K. Tung, JHEP **02**, 032 (2006).
- [57] R. Bonciani and A. Ferroglia, (2009), arXiv:0909.2980.
- [58] N. Kidonakis, Phys. Rev. **D75**, 071501 (2007).
- [59] G. Bordes and B. van Eijk, Nucl. Phys. **B435**, 23 (1995).
- [60] T. Stelzer, Z. Sullivan, and S. Willenbrock, Phys. Rev. **D56**, 5919 (1997).
- [61] T. Stelzer, Z. Sullivan, and S. Willenbrock, Phys. Rev. **D58**, 094021 (1998).
- [62] T. M. P. Tait, Phys. Rev. **D61**, 034001 (2000).
- [63] J. M. Campbell, R. Frederix, F. Maltoni, and F. Tramontano, (2009), arXiv:0907.3933.
- [64] S. Heim, Q.-H. Cao, R. Schwienhorst, and C. P. Yuan, (2009), arXiv:0911.0620.
- [65] A. Djouadi, J. Kalinowski, and M. Spira, Comput. Phys. Commun. **108**, 56 (1998).
- [66] M. L. Mangano, M. Moretti, F. Piccinini, R. Pittau, and A. D. Polosa, JHEP **07**, 001 (2003).
- [67] C. Kao, S. Sachithanandam, J. Sayre, and Y. Wang, (2009), arXiv:0908.1156.
- [68] S. Dawson, C. B. Jackson, L. Reina, and D. Wackerroth, Mod. Phys. Lett. **A21**, 89 (2006).
- [69] S. Yang, (2009), arXiv:0904.1646.
- [70] D0, V. M. Abazov *et al.*, Phys. Rev. Lett. **96**, 011801 (2006).

- [71] O. J. P. Eboli and D. Zeppenfeld, Phys. Lett. **B495**, 147 (2000).
- [72] J. R. Ellis, M. K. Gaillard, and D. V. Nanopoulos, Nucl. Phys. **B106**, 292 (1976).